Sensitivity analysis of time-lapse images obtained by differential waveform inversion with respect to reference model

Amir Asnaashari [†*], *Romain Brossier* [†], *Stéphane Garambois* [†], *François Audebert* [‡], *Pierre Thore* [‡], *and Jean Virieux*[†]
[†] *Institut des Sciences de la Terre (ISTerre), Université Joseph Fourier & CNRS*
[‡] *TOTAL E&P*

SUMMARY

For monitoring purposes, one of the promising techniques dedicated to assess physical properties changes in target regions is the differential waveform inversion, both in the acoustic and elastic cases. A central question of this technique regards the choice of the reference model. One solution could be the use of the reconstructed baseline image provided through the standard Full Waveform Inversion (FWI) procedure of initial data. However, how the accuracy of the baseline reconstructed image will affect the precision of further time-lapse images is of crucial importance. Here, we present a sensitivity analysis of time-lapse images obtained from differential inversion, with respect to various reference models. Density, P- and S-wave velocity changes could be converted into fluid property changes thanks to an empirical downscaling relationship. For accurate estimation of fluid parameter changes, the construction of highly resolved time-lapse images presenting acceptable errors is a key issue for the downscaling procedure. We illustrate on a specific synthetic example that the sensitivity analysis over the reference model variation provides linear convergence towards the time-lapse image obtained when using the exact baseline. An accurate baseline reconstruction is essential and could benefit from other data collected for monitoring purposes.

INTRODUCTION

FWI is a data fitting procedure aiming to develop high resolution quantitative images of the subsurface, through the extraction of the full information content of the seismic data (Tarantola, 1984). Beside the exploration application, the FWI method can be also used for monitoring applications, such as oil and gas reservoirs, steam injection, CO_2 sequestration, in order to obtain a quantitative image of changes of physical properties in target regions from successive seismic experiments.

The conventional difference method for time-lapse inversion needs to independently invert the two data sets (baseline and monitor sets) and to subtract the final derived monitor model from that of the baseline one in order to obtain a perturbation image of property changes (Plessix et al., 2010). This procedure might not be so robust because spurious features on both baseline and monitor images could potentially contaminate the differential model.

An alternative strategy consists in inverting only the differential data set to recover a differential image. The differential (double difference) method is widely used in geodesy and in seismology in order to improve earthquake source locations or to image receiver areas (Monteiller et al., 2005). This procedure has been proposed for time-lapse waveform inversion of acoustic data in frequency domain (Watanabe et al., 2004) and inversion of elastic data in time domain (Denli and Huang, 2009). The main advantage of the differential method compared to the difference approach is that the common noise between surveys can be rejected by data differentiation (Watanabe et al., 2004). The final time-lapse image is then more robust to noise contamination.

In this study, we investigate the influence of the reference model on the quality of the time-lapse V_p reconstruction by differential acoustic FWI. In particular, we address the required accuracy of the V_p reference model to delineate high resolution time-lapse image of steam injection in the acoustic version of the Dai et al. (1995) model.

STANDARD FULL WAVEFORM INVERSION

Standard FWI is an iterative optimization problem that is generally introduced as a linearized least-squares problem which attempts to minimize the residuals between the observed and the modeled wavefields (Tarantola, 1987). The inverse problem can be formulated in the frequency domain (Pratt and Worthington, 1990), and the associated objective function to be minimized is defined by

$$\mathscr{C} = \sum_{if=1}^{nf} \sum_{is=1}^{ns} \frac{1}{2} \Delta \mathbf{d}^{\dagger} \Delta \mathbf{d}, \tag{1}$$

where the data misfit error $\Delta \mathbf{d} = \mathbf{d}_{obs} - \mathbf{d}_{calc}$ denotes the difference between the observed data $\mathbf{d}_{obs}$ and the modeled data $\mathbf{d}_{calc}$ computed in the model $\mathbf{m}^{(n)}$ at the iteration n of the inversion. Superscript † indicates the adjoint (transposed conjugate). The summations in equation (1) are performed over the ns sources and a group of nf simultaneously inverted frequencies. The synthetic data $\mathbf{d}_{calc}$ is obtained by applying a sampling operator $\mathbf{S}$ to the incident wavefield $\mathbf{u}$ resulting from the forward problem resolution $\mathbf{A}\mathbf{u} = \mathbf{s}$, where the impedance matrix $\mathbf{A}$ is the forward problem operator and $\mathbf{s}$ represents the source term.

The gradient $\mathscr{G}$ of the objective function with respect to the model parameters $\mathbf{m} = \{m_i\}_{i=1,N}$, where N denotes the number of unknowns, can be derived from the adjoint-state formulation using the back-propagation technique (Plessix, 2006). This formulation gives for the i^{th} component of the gradient $\mathscr{G}$:

$$\mathscr{G}_{m_i} = \sum_{if=1}^{nf} \sum_{is=1}^{ns} \Re \Big\{ \mathbf{u}^t \frac{\partial \mathbf{A}^t}{\partial m_i} \lambda^* \Big\}, \tag{2}$$

where ^{t} and * denote the transpose and conjugate operators, respectively, and $\Re$ denotes the real part of a complex number. The gradient can be computed as a product between the incident wavefield $\mathbf{u}$ from the source, and the adjoint back-propagated

wavefield λ^* which is computed as $\mathbf{A}\lambda^* = \mathbf{S}^t\Delta\mathbf{d}^*$, using residuals at receiver positions as a composite source. Therefore, for computing gradient, only two forward problems per shot are required. The radiation pattern of the scattering by the model parameter m_i is represented by the sparse matrix $\partial\mathbf{A}/\partial m_i$.

The gradient of the objective function is then used in an optimization algorithm to update the model vector with the perturbation vector $\delta\mathbf{m}^{(n)}$ through the expression

$$\mathbf{m}^{(n+1)} = \mathbf{m}^{(n)} + \alpha^{(n)}\delta\mathbf{m}^{(n)}, \tag{3}$$

where the step length at iteration n is denoted by $\alpha^{(n)}$. In this study, a quasi-Newton L-BFGS (Nocedal, 1980) optimization scheme with line search is used in the FWI algorithm (Brossier, 2011).

DIFFERENTIAL WAVEFORM INVERSION

In differential method, instead of minimizing the difference between observed and computed data, we attempt to minimize the difference of the differential data between two sets of data (Watanabe et al., 2004; Denli and Huang, 2009), giving us the expression

$$\Delta\mathbf{d} = (\mathbf{d}_{obs_{monitor}} - \mathbf{d}_{obs_{baseline}}) - (\mathbf{d}_{calc_{monitor}} - \mathbf{d}_{calc_{baseline}}), \tag{4}$$

where $\mathbf{d}_{obs_{monitor}}$ and $\mathbf{d}_{obs_{baseline}}$ are the observed data from monitor and baseline surveys respectively, and $\mathbf{d}_{calc_{monitor}}$ and $\mathbf{d}_{calc_{baseline}}$ are the computed data for these experiments.

For the differential analysis, we first need the construction of a composite data set defined as

$$\mathbf{d}_{composite} = \mathbf{d}_{obs_{monitor}} - \mathbf{d}_{obs_{baseline}} + \mathbf{d}_{calc_{ref}}, \tag{5}$$

which is composed of (a) the time-lapse differential observed data $(\mathbf{d}_{obs_{monitor}} - \mathbf{d}_{obs_{baseline}})$ which should only represent the time-lapse changes of the two data sets and (b) the simulated data $\mathbf{d}_{calc_{ref}}$ computed using forward modeling in one arbitrary reference model. This reference model should explain as much as possible the $\mathbf{d}_{obs_{baseline}}$ data. This composite data set $\mathbf{d}_{composite}$ can be used as a new observed data set $\mathbf{d}_{obs}$ in equation (1), which is now equivalent to minimize the differential residual (4) with a standard FWI algorithm.

The differential approach requires that the acquisition surveys of the two experiments match or could be matched easily to perform the difference of the data sets. It means that this method is dedicated to permanent monitoring systems, where sensors are deployed once and where the repeatability of the source should be somehow fulfilled. The meaning of such source repeatability is a question we shall not address here.

The full procedure of differential approach can be summarized in the algorithm 1. Results of this algorithm depend on the reference model and one may question the relation between the accuracy in the time-lapse image and the selection of the reference model.

Algorithm 1 Preprocessing and inversion procedure with the differential algorithm

1: Creating the reference model $\mathbf{m}_{ref}$
2: $\mathbf{d}_{calc_{ref}}$ are computed in $\mathbf{m}_{ref}$
3: The composite data $\mathbf{d}_{composite}$ are computed (equation (5))
4: A standard FWI procedure is used to invert $\mathbf{d}_{composite}$ data from the $\mathbf{m}_{ref}$ model that gives $\mathbf{m}_{composite}$
5: The time-lapse model changes $\delta\mathbf{m}_{timelapse}$ can be computed from model $\delta\mathbf{m}_{timelapse} = \mathbf{m}_{composite} - \mathbf{m}_{ref}$

SENSITIVITY ANALYSIS

Extracting porosity and saturation for reservoir modeling is one task of the time-lapse processes. A downscaling procedure is essential to get fluid property changes from seismic parameters P- and S-wave time-lapse images. In order to get accurate changes in fluid properties, reconstruction of highly resolved and accurate differential images is crucial.

One of the conditions that has an important effect on final time-lapse image is the reference model that is used for differential inversion. As for full waveform inversion, the starting model is a crucial point to ensure convergence toward the global minimum. However, in differential FWI for reservoir monitoring, the inversion procedure focuses only on the scattered wavefield due to the time-lapse changes of the reservoir target that affects mostly the high frequency content of the data. Therefore, because of this lack of low frequency content in the time-lapse data, the selection of the starting model is crucial for the quality of the time-lapse image.

The reconstruction of the baseline model through the application of a standard FWI to the baseline data set will provide one possible starting model. Is this model enough for accurate differential time-lapse imaging? In order to address this point, the sensitivity of time-lapse image with respect to the reference model is studied. Several differential inversions are performed using the same differential data set $(\mathbf{d}_{obs_{monitor}} - \mathbf{d}_{obs_{baseline}})$, but using different reference models. We vary these starting models from the FWI baseline model to the exact baseline model using a linear interpolation at each point of the medium.

The quality control of final images needs an objective criterion. Let us define the medium perturbation as

$$\delta\mathbf{m}_{composite} = \mathbf{m}_{composite} - \mathbf{m}_{true-baseline}, \tag{6}$$

where $\mathbf{m}_{composite}$ is the model parameter obtained by differential inversion of composite data set. Then, the misfit value between $\delta\mathbf{m}_{composite}$ and true time-lapse model changes can be computed using the expression

$$\varepsilon = \sqrt{\sum_{i=1}^{N}\left(\delta m_{i_{composite}} - \delta m_{i_{true-timelapse}}\right)^2}, \tag{7}$$

where N denotes the number of model unknowns. In order to have a better comparison, we normalize this misfit value using this equation,

$$\gamma = \frac{\varepsilon - \varepsilon_{min}}{\varepsilon_{max} - \varepsilon_{min}} \times 100, \tag{8}$$

where ε_{min} represents the minimum ε that can be achieved from differential inversion with the true baseline used as a reference model. The quantity ε_{max} indicates the maximum misfit value obtained from the FWI baseline model in our case. A second criterion is introduced for the analysis of the quality of the reference model through

$$\mu = \sqrt{\sum_{i=1}^{N} \left(m_{i_{ref}} - m_{i_{true-baseline}}\right)^2}, \tag{9}$$

where we normalize this model variation through the expression

$$\eta = \frac{\mu}{\mu_{max}} \times 100. \tag{10}$$

In equation (10), μ_{max} denotes the maximum misfit value obtained when considering the reconstructed baseline image.

The acceptable upper limit of the function η leads to time-lapse images with an acceptable accuracy for downscaling. For an estimation of this acceptable range, we have to consider the downscaling procedure for computing fluid properties through empirical relationship between macro-scale elastic parameters (like wave speed) and micro-scale properties related to fluid parameters. This range is highly dependent on the accuracy that we expect for computing fluid parameters, since the time-lapse model should be used to compute the changes in porosity, fluid saturation and pore pressure using this empirical relationship (Landrø, 2001).

Therefore, considering the required accuracy on fluid parameters like porosity, we can estimate the required accuracy on the macro-scale velocity time-lapse models. From the relation between time-lapse models accuracy / reference model accuracy, we can determine the required reference model for differential FWI procedure to ensure a robust work-flow from time-lapse composite data until microstructure characterization.

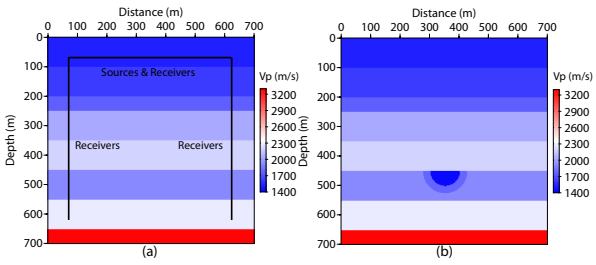

Figure 1: True V_p models: (a) the baseline, (b) the monitor.

SYNTHETIC APPLICATION

We assess the previous methodology on a synthetic example. We considered an acoustic synthetic version of the field example provided by Dai et al. (1995). The true P-wave velocity models for our acoustic time-lapse analysis are shown in Figure 1. Baseline model consists of eight layers; the sixth one is saturated with oil. After steam injection into this layer, the heat leads to two concentric areas at depth of 450 m, one saturated with steam and the outer one with heated oil.

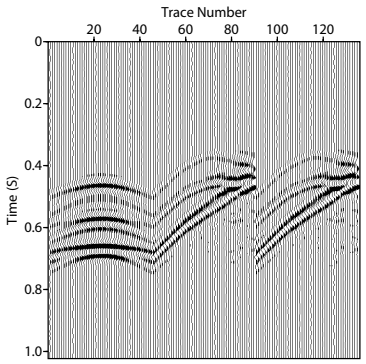

Figure 2: Differential seismogram of pressure data for the source located at the center $x = 350\ m$.

Our time-lapse configuration considers 23 sources, located along a horizontal line with interval of 25 m, below the surface at 75 m depth. We consider one line of receivers at the same depth as the sources and two vertical lines of receivers inside two boreholes at $x = 75\ m$ and $x = 625\ m$. An explosive Ricker source with a central frequency of 20 Hz is used for all shots. The time seismograms in baseline and monitor models are generated using a P_0 finite element Discontinuous Galerkin forward modeling (Brossier, 2011) and Perfectly-Matching-Layer absorbing boundaries condition all around the model. For all FWI tests, we use the same set-up and invert the data sets between $10-60$ Hz using sequential inverted frequencies with the inversion algorithm proposed by Brossier et al. (2009).

The baseline data set is first inverted through standard FWI to reconstruct the baseline image. Then, using linear interpolation between this reconstructed model and the true baseline model, three other models are created. Thus we ended up testing five reference models: the FWI baseline model (Figure 4.a), the true baseline model (Figure 4.e), and three intermediate models (Figure 4.b-d). These five reference models are used as an initial model for the differential inversion of differential data set (Figure 2) to study the sensitivity of time-lapse image. The normalized error γ (equation (8)) for time-lapse images is computed for each result, and these error values are plotted, in Figure 3, versus the accuracy of the reference model described by the parameter η.

The results and sensitivity curve show that the quality of the reference model directly drives the quality of the time-lapse image, what we expected. A linear relation also appears in Figure 3, meaning that the time-lapse imaging in this case can be related to a linear regime of the inversion. From downscaling constraints and Figure 3, we can determine the required accuracy of the reference model for micro-scale characterization.

In addition, it should be mentioned that reconstruction of the baseline model from standard FWI only could potentially not be sufficient for being used as a reference for differential inversion. However, for monitoring purposes, extra-information can be used like well data and geological constraints. These data should be used as a priori information in the framework of constrained FWI in order to build high resolution baseline models

for time-lapse imaging.

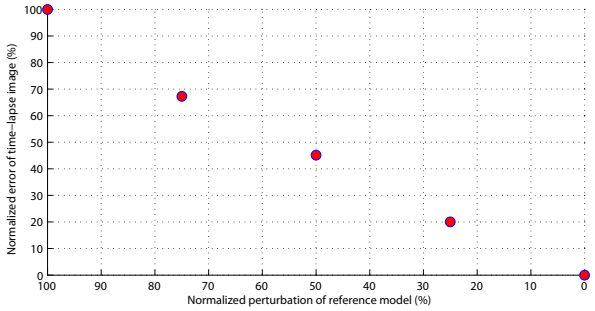

Figure 3: Sensitivity curve. Vertical axis indicates the γ value and horizontal one denotes the value of η. $\eta = 100\%$ and $\eta = 0\%$ represent the cases i) when the reconstructed baseline image through standard FWI, and ii) when the true baseline are respectively used as reference models.

CONCLUSIONS

We have studied the sensitivity of P-wave time-lapse imaging in terms of reference model accuracy for differential waveform inversion. Through a synthetic test, we have illustrated the relation between reference model accuracy and time-lapse image accuracy. This relation can be used to determine the required accuracy on the reference model in the framework of downscaling procedure for fluid characterization in reservoirs. This accuracy of reference model in differential approach is much more important than in standard full waveform inversion, since the inversion focuses on time-lapse response that affect mostly the high frequency content of the data. We propose that this level of accuracy of the reference model cannot be reached from standard FWI of recorded seismic baseline data only, but should benefit from available a priori information like well data and geological constraints. It will allow better building the accurate reference model from constrained FWI.

Perspectives of the work will focus on visco-elastic differential FWI and target oriented imaging on synthetic and real data.

ACKNOWLEDGMENTS

This study has been funded by TOTAL Exploration & Production. This work was performed using HPC resources from GENCI-CINES (Grant 2010-046091).

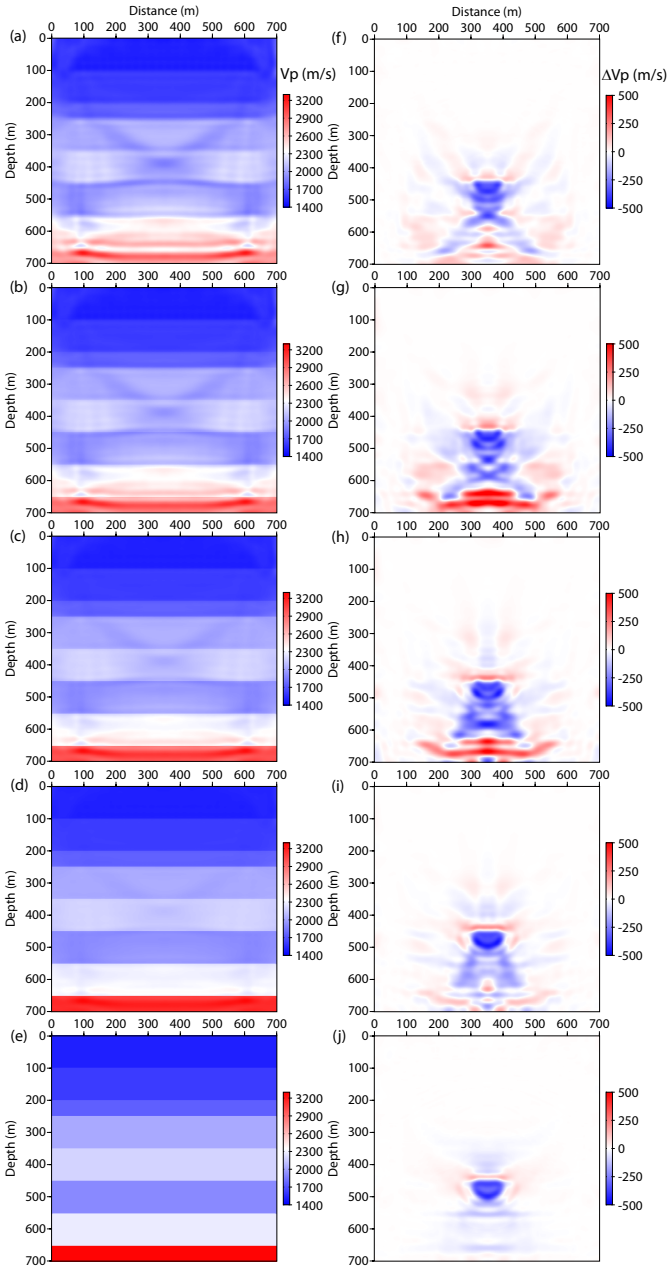

Figure 4: Reference and time-lapse V_p models: left panel shows the evolution of reference models from (a) reconstructed baseline image to (e) the true baseline model, and right panel illustrates each time-lapse image corresponding to the reference model at the left part.

EDITED REFERENCES

Note: This reference list is a copy-edited version of the reference list submitted by the author. Reference lists for the 2011 SEG Technical Program Expanded Abstracts have been copy edited so that references provided with the online metadata for each paper will achieve a high degree of linking to cited sources that appear on the Web.

REFERENCES

Brossier, R., 2011, Two-dimensional frequency-domain viscoelastic full waveform inversion: Parallel algorithms, optimization and performance: Computers & Geosciences, **37**, no. 4, 444–455, doi:10.1016/j.cageo.2010.09.013.

Brossier, R., S. Operto, and J. Virieux, 2009, Seismic imaging of complex onshore structures by 2D elastic frequency-domain full-waveform inversion: Geophysics, **74**, no. 6, WCC105–WCC118, doi:10.1190/1.3215771.

Dai, N., A. Vafidis, and E. Kanasewich, 1995, Wave propagation in heteregeneous porous media: A velocity-stress, finite-difference method: Geophysics, **60**, 327–340, doi:10.1190/1.1443769.

Denli, H., and L. Huang, 2009, Double-difference elastic waveform tomography in the time domain: 79th Annual International Meeting, SEG, Expanded Abstracts, 2302–2306.

Landrø, M., 2001, Discrimination between pressure and fluid saturation changes from time-lapse seismic data: Geophysics, **66**, 836–844, doi:10.1190/1.1444973.

Monteiller, V., J.-L. Got, J. Virieux, and P. Okubo, 2005, An efficient algorithm for double-difference tomography and location in heterogeneous media, with an application to the Kilauea volcano: Journal of Geophysical Research, **110**, B12, B12306, doi:10.1029/2004JB003466.

Nocedal, J., 1980, Updating quasi-Newton matrices with limited storage: Mathematics of Computation, **35**, no. 151, 773–782, doi:10.1090/S0025-5718-1980-0572855-7.

Plessix, R.-E., 2006, A review of the adjoint-state method for computing the gradient of a functional with geophysical applications: Geophysical Journal International, **167**, no. 2, 495–503, doi:10.1111/j.1365-246X.2006.02978.x.

Plessix, R.-E., S. Michelet, H. Rynja, H. Kuehl, C. Perkins, J. W. de Maag, and P. Hatchell, 2010, Some 3D applications of full-waveform inversion: Presented at the 72nd Annual International Conference and Exhibition, EAGE.

Pratt, R. G., and M. H. Worthington, 1990, Inverse theory applied to multisource crosshole tomography, Part I: Acoustic wave-equation method: Geophysical Prospecting, **38**, no. 3, 287–310, doi:10.1111/j.1365-2478.1990.tb01846.x.

Tarantola, A., 1984, Linearized inversion of seismic reflection data: Geophysical Prospecting, **32**, no. 6, 998–1015, doi:10.1111/j.1365-2478.1984.tb00751.x.

———, 1987, Inverse problem theory: Methods for data fitting and model parameter estimation: Elsevier.

Watanabe, T., S. Shimizu, E. Asakawa, and T. Matsuoka, 2004, Differential waveform tomography for time-lapse crosswell seismic data with application to gas hydrate production monitoring: 74th Annual International Meeting, SEG, Expanded Abstracts, 2323–2326.